JOURNAL OF GEOPHYSICAL RESEARCH, VOL. 101, NO. D22, PAGES 29,091–29,104, DECEMBER 20, 1996

# Transport of ozone and sulfur to the North Atlantic atmosphere during the North Atlantic Regional Experiment

Catharine M. Banic, W. Richard Leaitch, George A. Isaac, and Mark D. Couture

Atmospheric Environment Service, Downsview, Ontario, Canada

Lawrence I. Kleinman and Stephen R. Springston

Environmental Chemistry Division, Brookhaven National Laboratory, New York

J. Ian MacPherson

Institute for Aerospace Research, National Research Council, Ottawa, Canada

**Abstract.** The horizontal transport of $O_3$, $SO_2$, and non-sea-salt particulate $SO_4^=$ over the ocean near Nova Scotia, Canada, is determined from in situ measurements made during the 1993 North Atlantic Regional Experiment (NARE) summer intensive. The average mass of $O_3$ transported through an area 1 m in horizontal extent and 5 km in the vertical is 2.8 g $s^{-1}$, moving from west to east. Anthropogenic $O_3$ accounts for 50% of the transport below 1 km, 35-50% from 1 to 3 km, 25-50% from 3 to 4 km, and 10% from 4 to 5 km. The average mass of $SO_2$ and $SO_4^=$ transported through the same area is 50 mg S $s^{-1}$, moving from west to east. Eighty percent of the $SO_4^=$ and 55% of the $SO_2$ are transported above 1 km, with little transport of these species seen above 3 km. The anthropogenic input of $O_3$ and S to the North Atlantic atmosphere from the North American continent is estimated.

## 1. Introduction

Anthropogenic ozone, its precursors, sulfate aerosol, and $SO_2$ are transported eastward from North America over the North Atlantic Ocean. Aircraft measurements made in 1986 along the east coast of North America indicated that transport was occurring aloft [*Galloway and Whelpdale*, 1987]. Summertime measurements of $O_3$ made near the eastern coast of Canada with ozonesondes in 1991 [*Fehsenfeld et al.*, this issue (a)] and by aircraft in 1992 [*Berkowitz et al.*, 1995] have shown plumes of high $O_3$ transported aloft. The transport can have a significant impact on the oxidant levels and aerosol composition over the North Atlantic Ocean, and there is evidence that this impact may extend as far east as Europe [*Tarrason and Iversen*, 1992]. The North Atlantic Regional Experiment (NARE) was undertaken to improve our understanding of this transport [*Fehsenfeld et al.*, this issue (a), (b)].

As part of the summer 1993 NARE intensive the National Research Council of Canada DHC-6 Twin Otter aircraft was flown in the vicinity of Yarmouth, Nova Scotia (Figure 1). On 21 days between August 12 and September 8, $O_3$, $SO_2$, particulate $SO_4^=$, and aerosol particle number concentrations were measured at altitudes from approximately 0.03 to 3 or 5 km within a few kilometers of the coastal site at Chebogue Point (10 km south of Yarmouth), or over the ocean to the south within 50 km of the coast. In this paper, data from these profiles are used to quantify the horizontal transport of ozone and the major S species ($SO_2$ and non-sea-salt $SO_4^=$). The pollutant plumes observed in the vicinity of Chebogue Point maintained their identity over distances of hundreds of kilometers [*Daum et al.*, this issue].



Paper number 95JD03430.
0148-0227/96/95JD-03430$09.00

## 2. Method

### 2.1. Instrumentation

All measurements were made from the National Research Council of Canada Twin Otter aircraft. Typical flight speeds and climb rates were 60 and 3 m $s^{-1}$, respectively. One second resolution is used for all continuous measurements.

Continuous measurements of $O_3$ and $SO_2$ mixing ratios were obtained with TECO-49 UV absorption and TECO-43S analyzers, respectively. The analyzers were calibrated daily (through the aircraft inlet line) using a transfer standard traceable to the National Institute of Standards and Technology (NIST) for $O_3$ (range 0 to 150 ppbv), and a permeation tube dilution system for $SO_2$ (range 0.3 to 10 ppbv). Baseline checks for both species were made in level flight at a number of different altitudes by sampling ambient air through a charcoal filter for 5 to 10 min at a frequency of 2 to 3 times per hour. The detection level for $SO_2$ is 0.2 ppbv and the uncer-

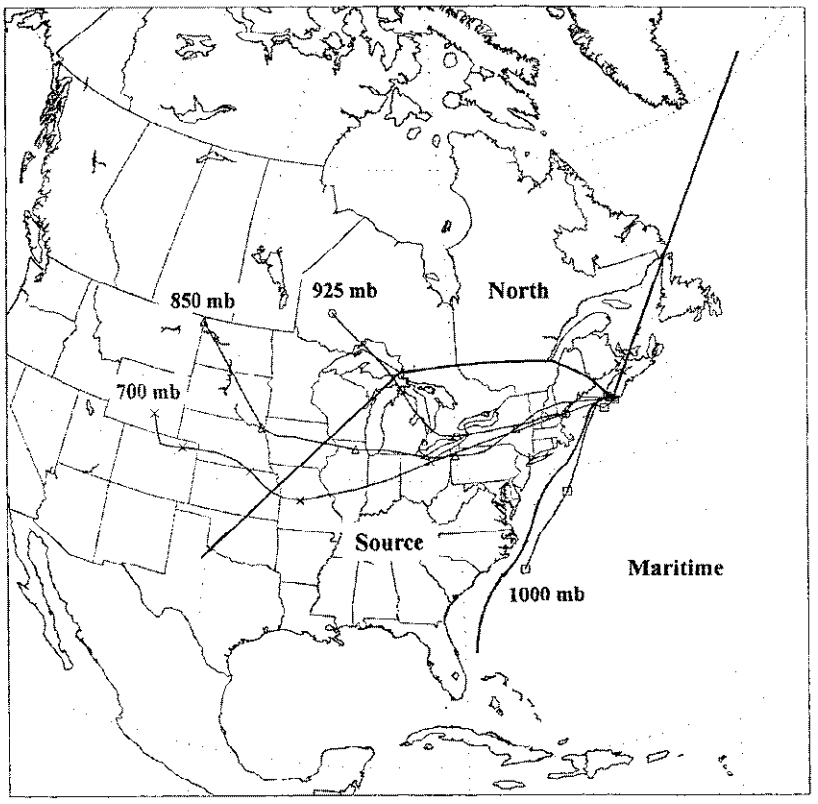


**Figure 1.** Sectors showing very low (maritime), low (north), and potentially high (source) regions of anthropogenic pollution. The 5-day back trajectories ending at Yarmouth are shown (24-hour markers) for 1800 UT on September 7, 1993.

tainties in the measurements are estimated at +/- (5 ppbv + 10%) for $O_3$ and +/- (0.1 ppbv + 30%) for $SO_2$. The inlet was a 0.8-cm (inner diameter) forward-facing Teflon line permitting fast transfer to the instrument. Response times were 20 s for $O_3$ and about 100 s for $SO_2$. Owing to the long response time, the $SO_2$ observations are smoother than the other measurements. The $SO_2$ data shown here have been shifted by 100 s. This shift has a minimal effect on the calculated transport, altering the integrated transport from 0 to 5 km by less than 1%, and the transport below 1 km by 4%.

Measurements of CO were made with a modified TECO 48 analyzer as described by *Kleinman et al.* [this issue (a)]. The CO averages given below are accurate to +/- (30 ppbv +15%).

Dried-aerosol number concentrations in 15 size bins covering the range 0.12 to 3.0 $\mu$m were measured continuously using a Particle Measuring Systems passive cavity aerosol spectrometer probe (PCASP-100X). Concentrations of particulate $SO_4^=$ were determined from analysis of aerosol collected on Teflon filters, each exposed in level flight in cloud-free air at a single altitude between 0.3 and 3 km for approximately 45 min. In general, one filter was exposed per flight. The filter inlet was stainless steel, forward-facing, smooth and with a diffuser nozzle permitting nearly isokinetic flow. Further details of the filter sampling times and altitudes, and analysis are given by *Li et al.* [this issue]. The contribution of sea-salt $SO_4^=$ was less than 1% of the total particulate $SO_4^=$.

Wind speed and direction were determined using a noseboom-mounted Rosemount 858 5-hole probe and a Litton 90-100 Inertial Reference System. Any bias in mean winds is less than 0.1 m $s^{-1}$, and the random error is less than 1 m $s^{-1}$ [*Angevine and MacPherson*, 1995]. Temperature and dew point were determined from a Rosemount 102DJICG heated fast-response probe, and an EG&G Model 137-S10 chilled mirror sensor, respectively.

### 2.2. Estimation of Sulfate Mass

Direct measurements of sulfate mass aloft are relatively sparse due to the long integration times needed to collect a sample. In contrast, aerosol particle concentration measurements are available at 1-s time resolution. Various relationships between the aerosol particle number concentration averaged over the times of filter collection and the non-sea-salt $SO_4^=$ (hereafter $SO_4^=$) mass as measured on the filters during NARE were investigated. The strongest relationship, shown in Figure 2, is

$$SO_4^= = 0.0907\ (PC7) - 1.126$$

where $SO_4^=$ is in micrograms per cubic meter, and PC7 (the PCASP number concentration measured in channel 7, corresponding to particles 0.3 to 0.4 $\mu$m in diameter) is in number per cubic centimeter. This relationship is strong enough ($R^2$ = 0.97) to use PCASP data as a continuous surrogate for the $SO_4^=$ mass. For PC7 $<13$ $cm^{-3}$, where the relationship would indicate a negative mass, sulfate mass is set to zero. The linear fit shown in Figure 2 may not be the best fit for the data at low $SO_4^=$ concentrations, but it is the best representation for the plumes.

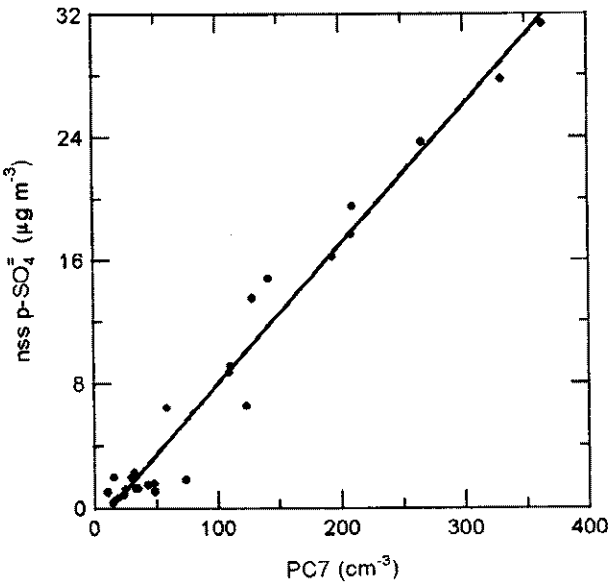


**Figure 2.** The relationship between the NARE 1993 Teflon filter non-sea-salt p-$SO_4^=$ and the particle number concentration in channel 7 of the PCASP. All values are at 1 atm, 0°C.

### 2.3. Selection of Profiles

The profiles used for the calculation of horizontal transport are described in Table 1. All profiles were taken over the ocean or near the coast at Chebogue Point and had $O_3$, $SO_2$, and PC7 data through a vertical depth exceeding 2.5 km. As Table 1 indicates, there were 15 days with one profile and 6 days with two profiles that met the data acceptance criteria. The results for horizontal transport presented here are calculated using a single profile per day (specified in Table 1 as set 1). As a sensitivity check, the analysis was repeated for all days, with the second profile of the day, generally having less data coverage and specified as set 2 in Table 1, substituted for that day. The differences in the magnitude of the average horizontal transport calculated for the altitude band of full data overlap (0 to 3 km) were found to be 5%, 2%, and <1% for $O_3$, $SO_2$, and $SO_4^=$, respectively. The direction of transport was insensitive to the choice of profiles.

During this intensive the Twin Otter made 48 flights, only 28 of which are included in Table 1. The remaining flights took place over land or through narrower altitude ranges to study specific features in more detail. The additional data generated by these flights are not shown in this paper, but do demonstrate a persistence in the features observed throughout the day, even on occasion from day to day. The calculation of

**Table 1.** Profiles Used to Determine Horizontal Transport

| Date | Time, UT | Altitude, km | Flight | Set | Sector[a] |
|---|---|---|---|---|---|
| Aug. 12 | 17 | 5 | 06 | 1 | M |
| Aug. 13 | 18 | 5 | 09 | 1 | |
| Aug. 16 | 15 | 5 | 12 | 1 | N |
| Aug. 17 | 15 | 3 | 14 | 1 | |
| | 19 | 3 | 15 | 2 | |
| Aug. 18 | 16 | 3 | 16 | 1 | M |
| | 20 | 3 | 17 | 2 | M |
| Aug. 19 | 18 | 0.15-5 | 18 | 1 | M |
| Aug. 20 | 20 | 5 | 19 | 1 | S |
| Aug. 21 | 01 | 4 | 20 | 2 | S |
| Aug. 23 | 18 | 5 | 22 | 1 | |
| Aug. 24 | 14 | 5 | 23 | 1 | S |
| | 19 | 3 | 24 | 2 | S |
| Aug. 25[b] | 11,17 | 5 | 25,26 | 1 | S |
| Aug. 26 | 19 | 3 | 27 | 1 | N |
| Aug. 27 | 19 | 5 | 28 | 1 | |
| Aug. 28 | 13 | 3 | 29 | 1 | S |
| Aug. 31 | 17 | 4 | 32 | 2 | S |
| | 22 | 3 | 33 | 1 | S |
| Sept. 01 | 20 | 3 | 35 | 1 | S |
| Sept. 02 | 14 | 3 | 36 | 1 | |
| Sept. 03 | 16 | 3 | 37 | 1 | S |
| Sept. 04 | 19 | 3 | 40 | 1 | S |
| Sept. 06 | 18 | 3 | 44 | 1 | S |
| Sept. 07 | 16 | 5 | 45 | 1 | S |
| | 19 | 5 | 46 | 2 | S |
| Sept. 08 | 13 | 3.4 | 48 | 1 | S |

The approximate time and maximum altitude are given. The minimum altitude is approximately 30 m unless otherwise shown.

[a] Maritime (M), north (N), source (S) as defined in section 2.2.

Calculations include all set 1 profiles. The calculation of transport with set 2 profiles substituted for set 1 are given in the text.

[b] Partial data for two flights combined to complete a single profile.

transport is made with measurements made in the afternoon. The air masses sampled had transport times of up to 4 or 5 days from the source regions [*Kleinman et al.*, this issue (b)], indicating that the air was subject to the full range of processes which could occur throughout the full 24-hour day.

The profiles of Table 1 were grouped by source region in order to demonstrate the differences in air originating over the source regions of pollutants in North America and air from the less-impacted regions. Back trajectories were calculated using the three-dimensional method of *Olson et al.* [1978] for every 0000, 0600, 1200, 1800 UT for the period August 1 through September 8, 1993, for air reaching Chebogue Point at 1000, 925, 850, and 700 mbar. The trajectory for the time closest to the time of the profile was selected as representative of the profile. Three sectors were defined as shown in Figure 1: maritime, north, and source. These sectors are characterized as very low, low, and potentially high anthropogenic pollution source regions, respectively [*Isaac et al.*, 1990; *Benkovitz et al.*, 1994]. For each level, each back trajectory was categorized by sector for three time periods: 0 to 24, 24 to 48, 48 to 72 hours. To be included in the source sector, air had to pass through the sector at any time during the 24-hour period. If the source sector was not encountered, the 24-, 48-, or 72-hour marker was used to classify the sector as north or maritime. Profiles were classified as maritime, north, or source if eight out of a possible nine sector indicators (24-, 48-, and 72-hour for each of 700, 850, and 925 mbar) were of a single type. Profiles with less than eight indicators from the same sector have a complex vertical structure reflecting the different sources of air and were not classified according to this scheme, but are included in the calculation of horizontal transport. Table 1 shows that 4, 2, and 15 profiles were classified as maritime, north, and source sectors, respectively, with six profiles unclassified. This represents 3, 2, 11, and 5 days of sampling, respectively.

### 2.4. Calculation of the Horizontal Transport

The data for each profile in Table 1 were averaged in 5-m intervals in the vertical to account for variable climb rates. The $O_3$ and $SO_2$ mixing ratios, and PC7 were converted to mass per unit volume for the in situ temperature and pressure conditions. For $SO_2$ mixing ratios less than the detection limit of 0.2 parts per billion per volume (ppbv), the $SO_2$ concentration was set to zero. The 5-m averages were used to calculate the horizontal transport for each profile. The horizontal transport, a vector quantity, has magnitude calculated as the product of the wind speed and the mass per unit volume, and direction given by the wind direction. The transport vector in each 5-m interval is resolved into east-west and north-south components, which are added over 100-m altitude bands. The average east-west and north-south components in each 100-m altitude band are determined, and used to calculate multiprofile averages. Owing to flight limitations, the average transport for the range 30 to 100 m is used to represent the full 0- to 100-m band. Transport through altitude ranges of 1 km or more is determined from the sum of the 100-m components. The vector components are recombined for the final transport numbers.

The weather in southern Nova Scotia during the NARE intensive was mainly clear and sunny, with many instances of fog or low stratus over the water and convective cloud, sometimes accompanied by showers, over land. The profiles of Table 1 were largely taken in clear air, but clouds a few hundred meters thick were encountered on six days (September 2 through 8). The clouds sampled ranged from surface fog, to stratus topped below 750 m, or layers topped at 1.5 to 3.0 km. An example from September 7, a day with fog and low stratus, is shown in Figure 3. Both $O_3$ and $SO_2$ are only weakly soluble [*Seinfeld*, 1986], but conversion of $SO_2$ to $SO_4^=$ in cloud water will deplete $SO_2$. Activation of aerosol particles in cloud reduces the aerosol particle number concentration, making the use of PC7 unsuitable for estimating $SO_4^=$. For in-cloud periods (defined as cloud droplet concentration greater than 10 $cm^{-3}$) the horizontal transport of $SO_4^=$ was calculated from the $SO_4^=$ determined in cloud water, using the measured cloud liquid water content to convert the aqueous phase concentrations to equivalent gas phase values (i.e., micrograms sulfur per cubic meter). The horizontal flux for $O_3$ and $SO_2$ is calculated in the same manner for in-cloud and clear periods. This procedure accounts for total S, with the exception of interstitial aerosol. Details of the cloud sampling are given by *Leaitch et al.* [this issue].

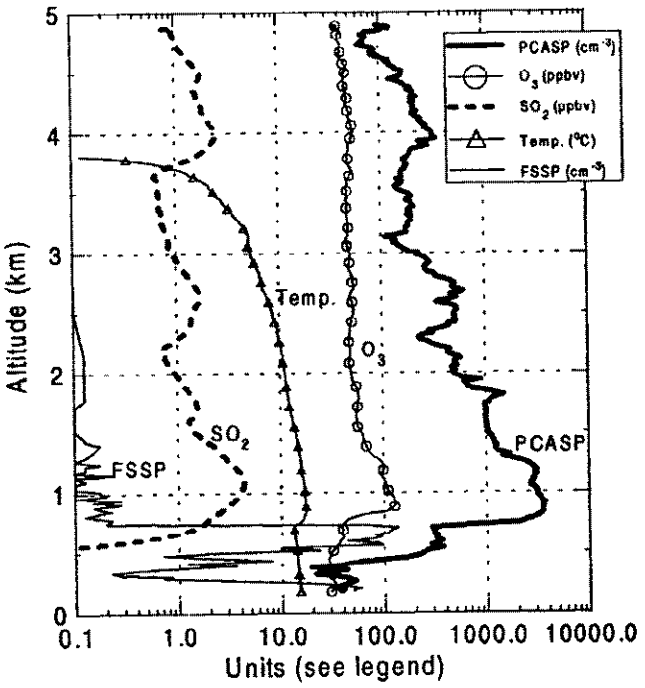


**Figure 3.** An ascent profile taken over Chebogue Point on September 7, 1993 (Flight 46). Wind direction was near 320° at the base of the profile, near 290° at 500 m, and 260° above 750 m. This example is for the same case as illustrated in Figure 1. The cloud droplet number concentration and aerosol number concentration are given by a Particle Measuring Systems forward scattering spectrometer probe (FSSP) and PCASP respectively.

## 3. Results and Discussion

### 3.1. Factors Influencing Transport

Table 2 shows the fraction of time air arriving in the study area at pressures down to 700 mbar, traversed a given sector 1, 2, or 3 days prior. Values for all 0000, 0600, 1200, 1800 UT from August 1 through September 8, 1993, are given.

**Table 2.** Percentage of Time Air Originated in a Given Sector

| | 700 mbar | 850 mbar | 925 mbar | 1000 mbar |
|---|---|---|---|---|
| | | *North* | | |
| 24 hours | 14 (14) | 19 (10) | 21 (14) | 13 (14) |
| 48 hours | 24 (19) | 25 (14) | 29 (19) | 11 (14) |
| 72 hours | 46 (52) | 36 (33) | 33 (29) | 21 (24) |
| | | *Maritime* | | |
| 24 hours | 18 (14) | 24 (24) | 31 (24) | 61 (71) |
| 48 hours | 10 (10) | 19 (19) | 21 (19) | 54 (62) |
| 72 hours | 3 (0) | 13 (14) | 19 (24) | 49 (48) |
| | | *Source* | | |
| 24 hours | 68 (71) | 57 (67) | 49 (62) | 26 (14) |
| 48 hours | 67 (71) | 56 (67) | 50 (62) | 35 (24) |
| 72 hours | 52 (48) | 51 (52) | 47 (48) | 30 (29) |

The values for 0000, 0600, 1200, 1800 UT from August 1 through September 8, 1993, are given, as well as only for the times of profiles used in the calculation of transport. The latter numbers are shown in parentheses.

These data show the high frequency of flow at 925 mbar and aloft from regions of potentially high anthropogenic impact, and the dominance of flow near the surface from the north and maritime regions. Since air arriving at 1000 mbar can be strongly decoupled from the air aloft, the 1000 mbar back trajectories were not considered in the sector assignment for profiles as given in Table 1. Table 2 also shows the back trajectory statistics for the times of the profiles used to calculate transport (i.e., the set 1 profiles in Table 1). The days sampled during the study closely represent the characteristics of the entire period.

One example of the effect of different origin for air at different altitudes is given in Figure 3. The back trajectories for this profile are given in Figure 1. The source sector air at 925, 850, and 700 mbar (approximately 0.75, 1.5, and 3 km) has much higher $O_3$ and $SO_2$ mixing ratios and aerosol particle concentrations than the maritime air near the surface. This strong decoupling will be evident in the following analysis.

In order to understand the transport occurring in this region, individual vertical profiles of wind speed and direction, and the thermodynamic tracer $\theta_q$ (adiabatic equivalent potential temperature: conservative for adiabatic expansion of moist air,

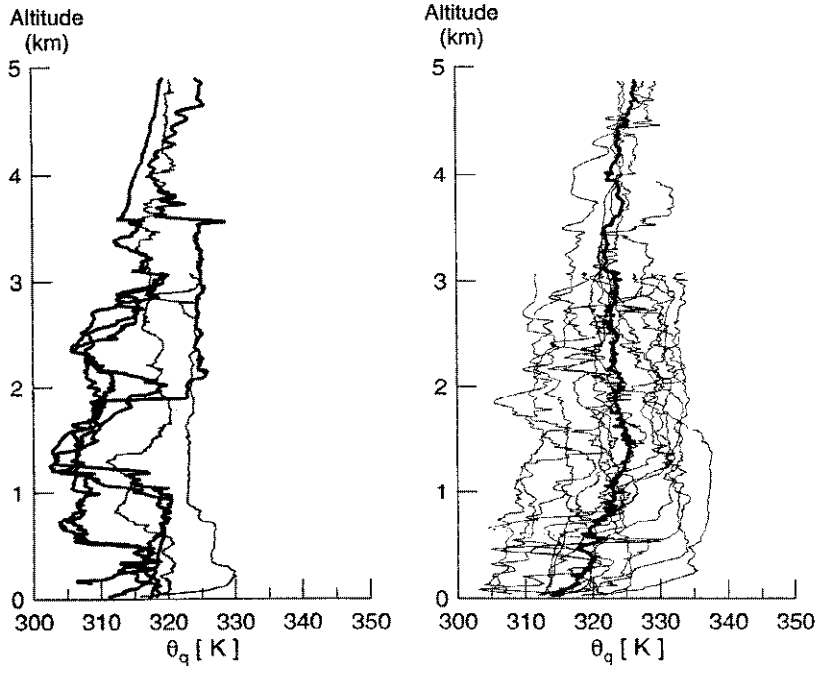


**Figure 4.** Potential temperature $\theta_q$ for the profiles shown in Table 1 for (left) maritime (heavy lines) and north (faint lines) sector cases, and (right) source cases (faint lines) and the average of the source cases (heavy line).

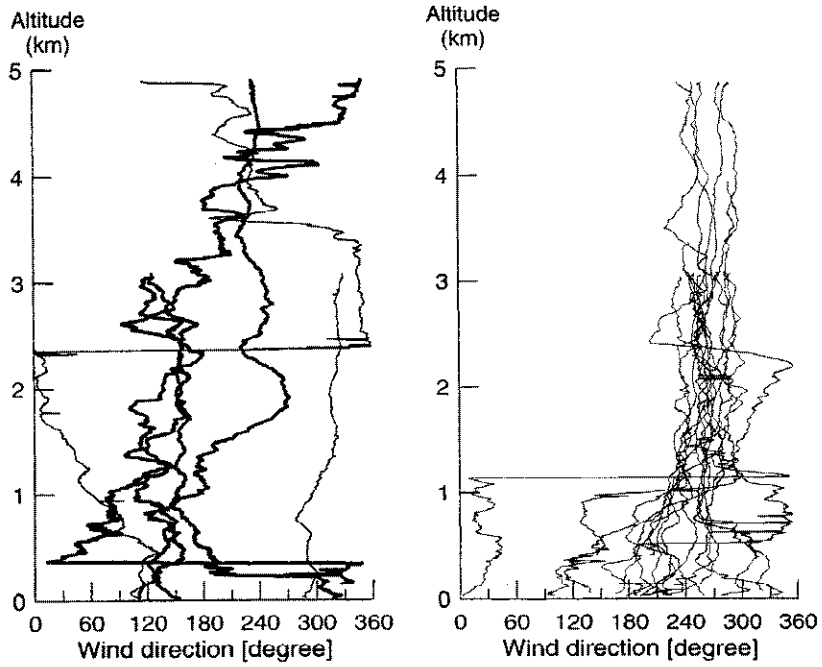


**Figure 5.** Wind direction relative to true north for the profiles shown in Table 1 for (left) maritime (heavy lines) and north (faint lines) sector cases, and (right) source cases (faint lines).

including condensation, evaporation and precipitation), as well as the $O_3$ and $SO_2$ mixing ratios and particle number concentrations were examined for each emission sector. Individual profiles indicate a high day-to-day variability, but similar trends are shared for air with a common emission history.

The variation in $\theta_q$ with altitude and sector is shown in Figure 4. The average $\theta_q$ for source sector profiles was constant near 322 K above 1 km, decreasing below 1 km to 315 K near 30 m, showing the inversion in the lowest 1 km. The north sector shows the surface inversion in the lowest 150 m. The maritime sector shows an inversion below 500 m. The greatest stability within the lowest 1 km of the atmosphere was seen for the average of the source sector profiles. This feature helps to initiate and maintain pollutant layers aloft [*Angevine et al.*, this issue].

The dependence of wind direction (relative to true north) on altitude and sector is shown in Figure 5. The local wind direction for air from the source sector varied considerably in

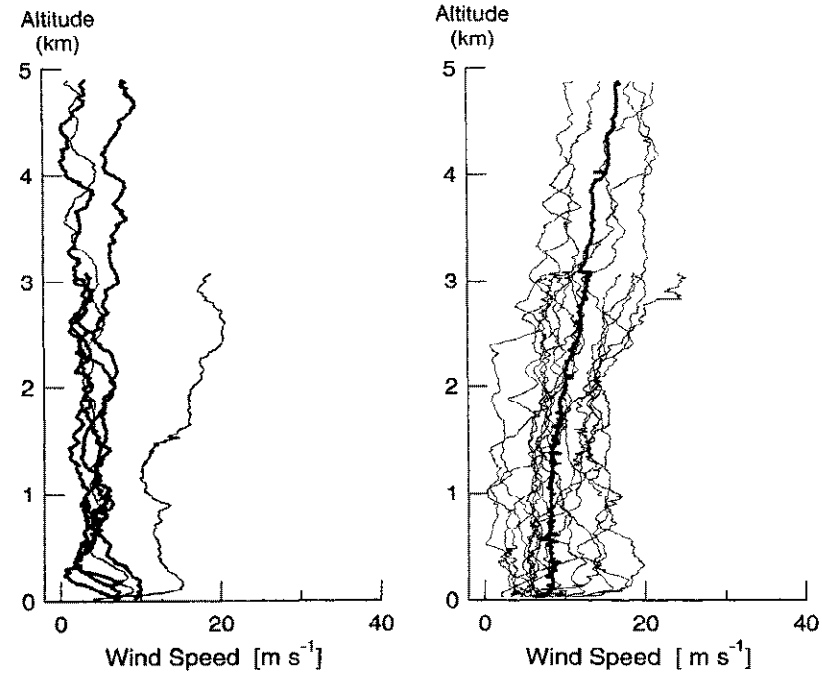


**Figure 6.** Wind speed for the profiles shown in Table 1 for (left) maritime (heavy lines) and north (faint lines) sector cases, and (right) source cases (faint lines) and the average of the source cases (heavy line).

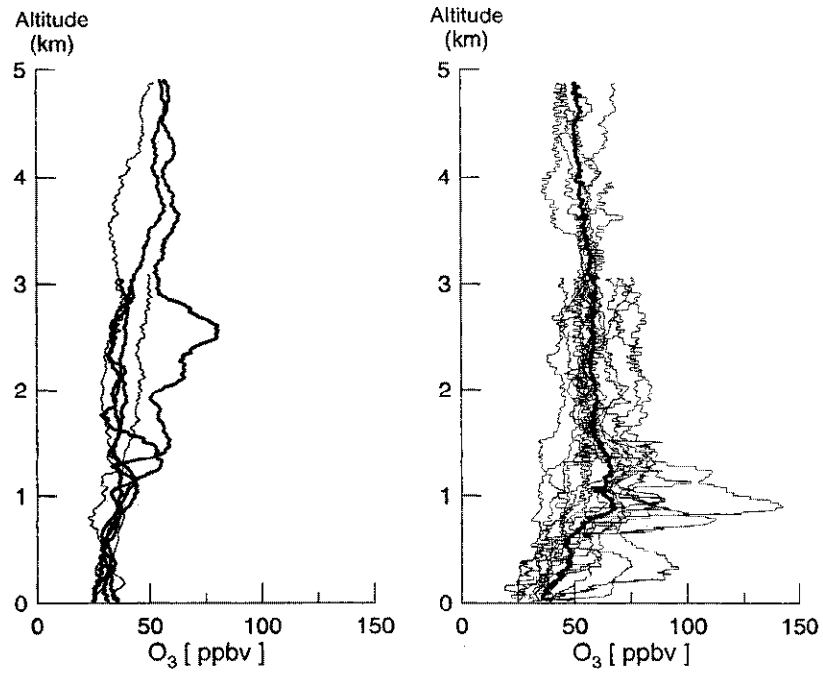


**Figure 7.** $O_3$ mixing ratios for the profiles shown in Table 1 for (left) maritime (heavy lines) and north (faint lines) sector cases, and (right) source cases (faint lines) and the average of the source cases (heavy line).

individual profiles below 1 km, but was most often near 250° at altitudes from 1 km to 5 km. Winds for north sector profiles were from the maritime or north sectors below 600 m and northerly aloft to 3 km. Maritime profiles showed winds from the north or maritime sectors below 600 m, and near 160° up to 3 km. Both north and maritime sectors showed westerly winds aloft, predominantly from 200° to 300° at 3 to 5 km.

The variation in wind speed with height is shown in Figure 6. On average the source sector wind speeds were 7 m $s^{-1}$ near 30 m, about 9 m $s^{-1}$ from 300 m to 2 km, and then increased steadily to 15 m $s^{-1}$ near 5 km. The north sector wind speeds were similar to the source sector or lighter. In contrast, the average maritime sector winds were 7 m $s^{-1}$ at 30 m and decreased rapidly within a few hundred meters altitude, with winds lighter than 10 m $s^{-1}$ aloft up to 5 km.

The $O_3$ mixing ratios for maritime, north, and source sector profiles are shown in Figure 7. The $O_3$ in maritime and north sector profiles was generally less than 50 ppbv from the surface

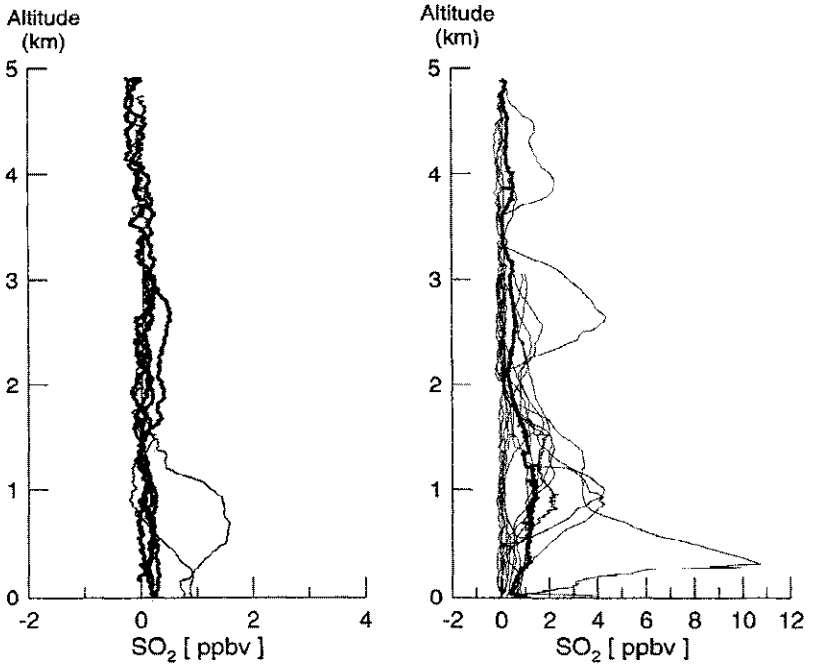


**Figure 8.** $SO_2$ mixing ratios for the profiles shown in Table 1 for (left) maritime (heavy lines) and north (faint lines) sector cases, and (right) source cases (faint lines) and the average of the source cases (heavy line).

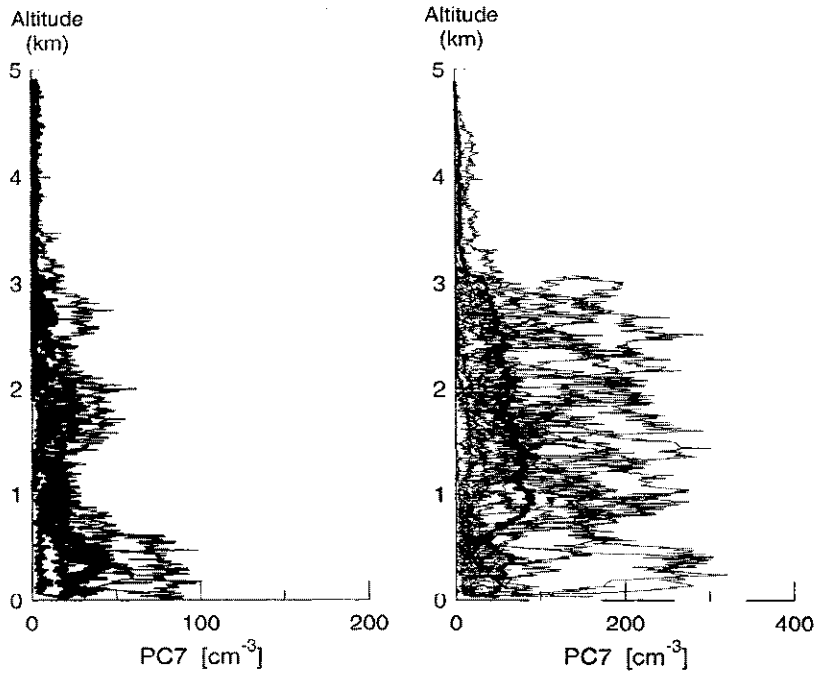


**Figure 9.** Concentrations of PC7 (the $SO_4^=$ surrogate) for the profiles shown in Table 1 for (left) maritime (heavy lines) and north (faint lines) sector cases, and (right) source cases (faint lines) and the average of the source cases (heavy line).

to 3 km, whereas the source sector average profile shows $O_3$ in excess of 50 ppbv from 600 m and up. Plumes of $O_3$ from 80 to 140 ppbv were seen at altitudes between 200 and 1300 m. Less $O_3$ is seen below 800 m, with the largest difference for the source sector profiles, reflecting the fact that north and maritime sector air could be seen near the surface when air from the source sector was aloft. The $O_3$ seen in the maritime and north sector profiles is used to estimate the nonanthropogenic (background) $O_3$.

The profiles of $SO_2$ mixing ratio are shown in Figure 8. Throughout the altitude range for maritime air, and above 2 km for north air, the $SO_2$ is near or below detection limit. Plumes of $SO_2$ are seen at low altitude for the north profiles, and throughout the altitude range for source sector air. The background value for $SO_2$ is considered to be below detection level.

The PC7, used as the surrogate for $SO_4^=$, are shown in Figure 9. In the maritime sector air concentrations as high as 45 $cm^{-3}$ are seen at altitudes up to 2 km, with values near 20 $cm^{-3}$ more common, as well as concentrations of less than 13 $cm^{-3}$ (the "detection level" for $SO_4^=$ from the relationship in 2.2 above) throughout the altitude range. North sector PC7 are typically near or below 50 $cm^{-3}$ above 600 m, and decrease to less than 10 $cm^{-3}$ above 3.5 km. Near the surface the concentrations reach 90 $cm^{-3}$, reflecting the fact that the north sector air aloft is decoupled from the sector of origin for air near the surface. In contrast, the source air can have particle concentrations in excess of 150 $cm^{-3}$ from the surface to 3 km, and the average particle concentration exceeds 50 $cm^{-3}$ from 0.6 to 2.5 km. The background value for $SO_4^=$ is taken as zero (i.e., PC7 = 13 $cm^{-3}$).

### 3.2. Horizontal Transport

The east-west and north-south components of the horizontal transport of $O_3$ for the maritime, north, and source sectors are shown in Figure 10. The average transport for all set 1 profiles is also shown. On the basis of the maritime and north profiles given in Figure 7, reasonable estimates of background ozone are 30, 40, and 50 ppbv, depending on altitude. To arrive at an estimate of the anthropogenic input, the horizontal transport was calculated after subtracting each of these values from the actual mixing ratios observed for each profile, setting negative $O_3$ mixing ratios to zero. The resulting average profiles are also shown in Figure 10. It is clear that the most significant transport of $O_3$ occurs to the east, with a component to the north at altitudes less than 2 km. The transport to the east increases with height, reflecting the general westerly winds seen, and the higher wind speeds aloft.

The east-west and north-south components of the flux of $SO_2$ for the maritime, north, and source sectors are shown in Figure 11. The average transport for all set 1 profiles is also given. Similar to $O_3$, there is considerable transport to the east, with some transport to the north seen below 2 km. The presence of sources of $SO_2$ in the north sector are indicated by the transport to the east and south for the north sector profiles. The contribution of maritime air to the transport of $SO_2$ is seen to be negligible.

The components of flux of $SO_4^=$ are shown in Figure 12, together with the average transport. Again, transport is mainly to the east, with a component to the north; the contribution of maritime air to the transport of $SO_4^=$ is negligible. There is a difference in the transport seen for the two S species: relatively more $SO_4^=$ is transported at higher altitudes than $SO_2$. The average transport profile for $H_2O$ (derived from the total mixing ratio = vapour + cloud liquid water content) is also shown in Figure 12. There is substantial eastward transport of $H_2O$ occurring at the same altitudes as $SO_4^=$, consistent with the results of *Kleinman and Daum* (1991). The transport of $H_2O$ from south to north is consistent with the ocean to the south acting as a source of water vapour.

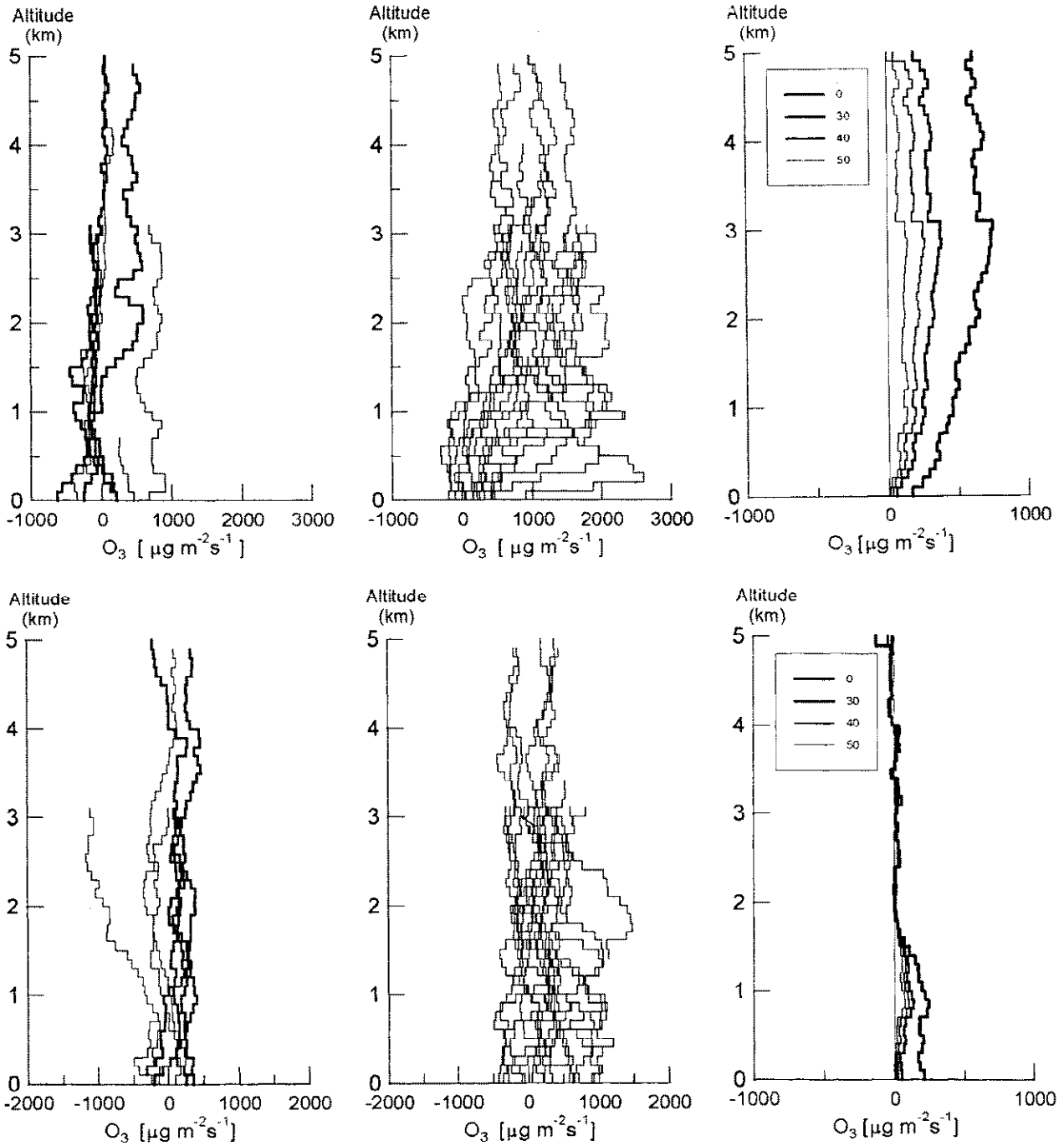


**Figure 10.** The (top panel) east-west and (bottom panel) north-south components of the flux of $O_3$, shown for (left, top and bottom) individual profiles for the maritime (heavy line) and north (faint line) sectors, (center, top and bottom) individual profiles for the the source sector, and (right, top and bottom) the average for all profiles of set 1. Transport to the east and north are shown as positive. Also given (right, top and bottom) are the average profiles with 30, 40, and 50 parts per billion by volume (ppbv) subtracted.

There are fewer days with data above 3 km than below for all species, and even fewer curves are evident for altitudes > 3 km for the S species. For many profiles the $SO_2$ and $SO_4^=$ transport above 3 km is zero, and for these profiles the curves lie along the axis. The loss of data coverage at 3 km causes a discontinuity in the average transport, which can be seen in Figures 10 through 12.

The mass of $O_3$ transported, both observed and after subtraction of 30, 40, or 50 ppbv, is given at 1-km resolution in Table 3. Application of the most reasonable background profile (30 ppbv below 1 km, 30 to 40 ppbv between 1 and 4 km, and 50 ppbv from 4 to 5 km) shows that 50% of the transport below 1 km, 35-50% of the transport from 1 to 3 km, 25-50% of the transport from 3 to 4 km, and 10% of the ozone transported from 4 to 5 km may be due to anthropogenic influence. These numbers suggest that the contribution of anthropogenic sources to transport above 5 km will be smaller than 10%. The direction of net transport, 240° for 0-1 km and

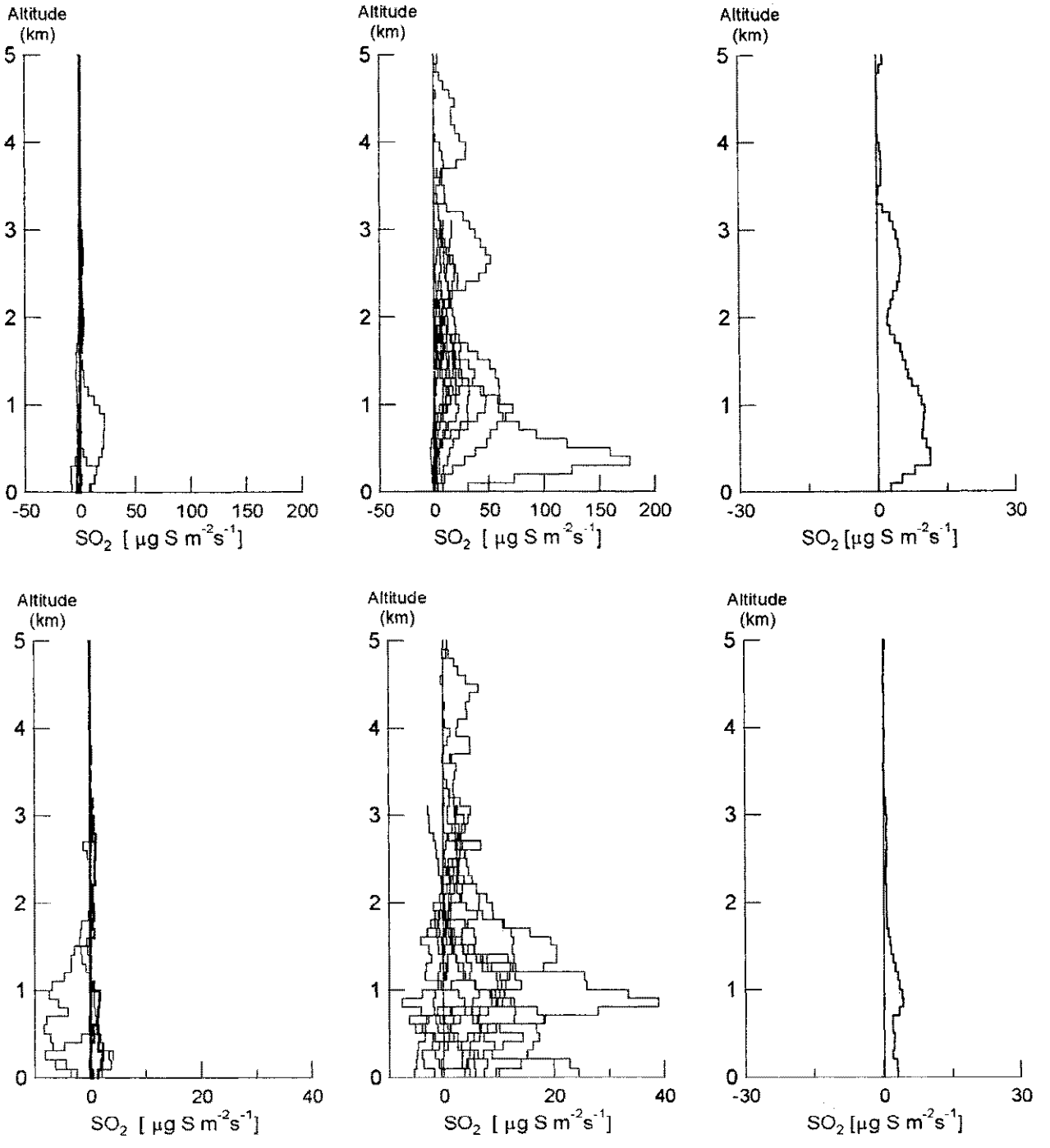


**Figure 11.** The (top panel) east-west and (bottom panel) north-south components of the flux of $SO_2$, shown for (left, top and bottom) individual profiles for the maritime (heavy line) and north (faint line) sectors, (center, top and bottom) individual profiles for the source sector, and (right, top and bottom) the average for all profiles in set 1. Transport to the east and north are shown as positive.

260° for 1-2 km for the observations, converges toward 253° (which is similar to the direction of transport of the S species) as progressively higher $O_3$ values are subtracted, shifting the weighting of the individual profiles more heavily to those with higher $O_3$ mixing ratio. Thus $O_3$ in plumes in excess of 50 ppbv is transported in the same direction as the S species, suggesting a common source region.

The mass of S transported as $SO_2$ and $SO_4^=$ is given at 1-km resolution in Table 3. The transport of $SO_2$ and $SO_4^=$ is considered to be very close to that due to anthropogenic input since background values for these species, assessed from consideration of the maritime profiles, are below or near detection level. The data of Table 3 show clearly that more $SO_4^=$ is transported at higher altitudes than $SO_2$, with only 21% of the mass of $SO_4^=$ transported below 1 km, relative to 45% of the $SO_2$. Both species show a very small contribution to transport above 3 km, and it is expected that very little S is transported above 5 km.

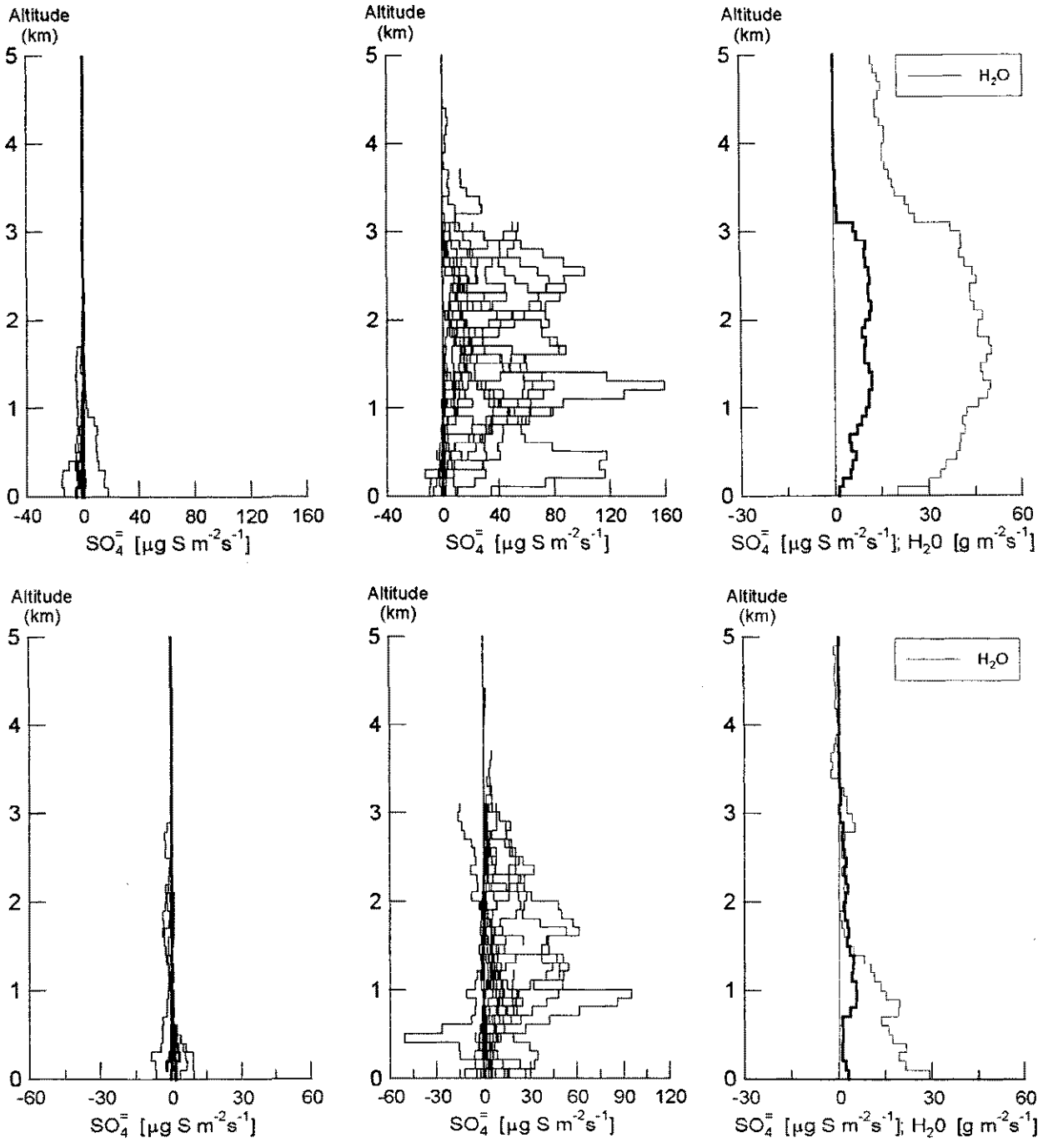


**Figure 12.** As Figure 11, but for $SO_4^=$. The average profile for $H_2O$ is also shown (right, top and bottom).

The transport of more $SO_4^=$ at higher altitudes than $SO_2$ is consistent with the fact that $SO_2$ is a primary pollutant with a surface-based source, which is gradually converted to $SO_4^=$ both in clear air and in cloud. Upward transport of both species can occur due to convective mixing of air over the continent. If convection is accompanied by the formation of clouds, $SO_2$ can be more rapidly oxidized to $SO_4^=$ by aqueous phase reactions in cloud water [*Liu et al.*, 1993; *Husain et al.*, 1991], and higher $SO_4^=$ relative to $SO_2$ would be seen at higher altitudes. The transport of $H_2O$ at the same altitudes as the $SO_4^=$ (Figure 12), is consistent with cloud processing of $SO_2$ to $SO_4^=$. The direction of the transport, after combination of the east-west and north-south components, is different for $SO_4^=$ and $H_2O$ because the spatial distribution of sources is different.

### 3.3. Seasonal Transport to the North Atlantic Atmosphere

Estimates of the transport of $O_3$ and S from the North American continent to the North Atlantic atmosphere can be made from the transport calculation given above. These estimates are compared with results in the literature.

The horizontal transport calculated here for the NARE intensive data set represents a snapshot of conditions over southern Nova Scotia in the summer. Similar investigations of the transport at other locations along eastern North America, or

**Table 3.** Mass of $O_3$, S, and $H_2O$ Transported in Each Altitude Range per Second per Meter of Horizontal Scale

| | | 0-1 km | 1-2 km | 2-3 km | 3-4 km | 4-5 km | 0-5 km |
|---|---|---|---|---|---|---|---|
| $O_3$ | mg $m^{-1}s^{-1}$ | 390 (239) | 530 (260) | 683 (269) | 650 (268) | 624 (273) | 2828 (264) |
| $O_3$ - 30 ppbv | mg $m^{-1}s^{-1}$ | 183 (245) | 274 (258) | 344 (267) | 298 (268) | 270 (275) | 1352 (264) |
| $O_3$ - 40 ppbv | mg $m^{-1}s^{-1}$ | 120 (247) | 188 (256) | 231 (266) | 183 (268) | 152 (278) | 862 (264) |
| $O_3$ - 50 ppbv | mg $m^{-1}s^{-1}$ | 76 (249) | 113 (253) | 123 (263) | 74 (269) | 63 (286) | 440 (262) |
| $SO_2$ | mg S $m^{-1}s^{-1}$ | 9.2 (253) | 5.9 (254) | 4.1 (263) | 1.2 (265) | 0.2 (259) | 20.6 (256) |
| $SO_4^=$ | mg S $m^{-1}s^{-1}$ | 5.9 (244) | 11 (252) | 11 (261) | 1.0 (265) | 0 | 28.6 (254) |
| $H_2O$ | kg $m^{-1}s^{-1}$ | 41 (242) | 48 (264) | 43 (267) | 21 (271) | 14 (274) | 165 (251) |

Note that $SO_2$ and $SO_4^=$ mass is expressed as S. The angle relative to true north, such that 270 is transport from west to east, is given in parentheses. The most reasonable estimates of transport of anthropogenic $O_3$, based on background profiles determined from north and maritime air, are underlined. For comparison the transport of water is also given.

at the same location in different seasons, may show differences [e.g., *Luria et al.*, 1987; *Luria et al.*, 1988; *Anderson et al.*, 1993]. However, modeling studies, such as by *Benkovitz et al.* [1994], support the approach taken below. It is recommended that the following analysis be strengthened by calculation of transport for the NARE period with data collected over distances of 1000 km by the other two research aircraft working in the vicinity [*Fehsenfeld et al.*, this issue (b)].

The distance scale chosen for this estimate is 2000 km (measured along a meridian) within which all the major emission regions lie. The timescales chosen are (1) the summer season (91 days), and (2) 1 year. For background $O_3$ of 30 ppbv from 0 to 1 km, 40 ppbv for 1 to 4 km, and 50 ppbv for 4 to 5 km, the average integrated transport from 0 to 5 km of $O_3$ due to anthropogenic sources was given in Table 3 to be 0.86 g $s^{-1}$ from 264° for each meter in the horizontal. This result, generalized over 2000 km, yields a flux of 14 Tg ( 300 billion moles) of anthropogenically produced $O_3$ per summer out to the North Atlantic atmosphere, suggesting that there is potentially more $O_3$ transported than the estimate of *Parrish et al.* [1993] of 100 billion moles per summer would indicate. *Parrish et al.* base their estimate on the relationship between $O_3$ and CO determined at a number of surface sites along eastern North America for all air masses in the summer of 1991. Figure 13 shows the relationship between $O_3$ and CO for source sector air below 2 km for the present study and the approximate envelope for measurements by *Parrish et al.* [1993] at Seal Island, Nova Scotia (within 100 km of the 1993 Twin Otter flight tracks). All data points from this study for altitudes less than 0.3 km lie within the envelope, but a larger number of data points at higher altitudes are seen to lie above the enve-

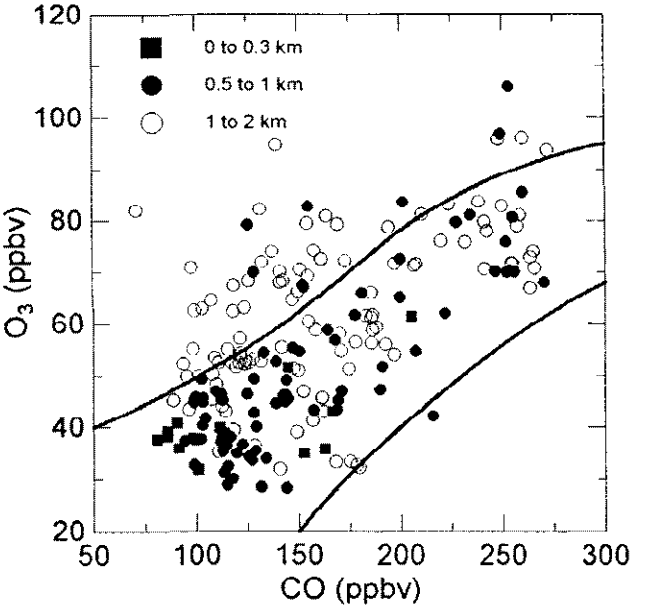


**Figure 13.** The relationship between $O_3$ and CO for source sector air below 0.3 km, from 0.5 to 1 km, and 1 to 2 km altitude. The lines show the envelope for the results of *Parrish et al.* [1993] for Seal Island for the summer of 1991. Averages of CO and $O_3$ over 100 m bins in the vertical are given for all source sector flights in Table 1, except 48 for which no data were available. Owing to changes in sector for near-surface air and air aloft, data have been suppressed for 0.3 to 0.5 km.

lope: 8 out of 78 data points from 0.5 to 1 km ... 47 out of 130 points from 1 to 2 km, also, not shown in Figure 13, 72 of 187 points from 2 to 5 km. For all altitudes combined only 1 point lies below the lower envelope. This indicates a trend to higher $O_3$ mixing ratios relative to CO aloft compared with the relationship observed at the surface.

The results of Table 3 give 49 mg S $s^{-1}$ for the eastward transport of S to the North Atlantic atmosphere through a surface 5 km high and 1 m wide. This result, generalized over 2000 km, gives 0.8 Tg S transported per summer. If the total transport of S is assumed to be constant for all seasons, the NARE result gives 3.2 Tg S $yr^{-1}$, consistent with the estimates of *Whelpdale and Galloway* [1994] of 3-4 Tg S $yr^{-1}$ being transported to the North Atlantic atmosphere.

## 4. Conclusions

The horizontal transport of $O_3$, $SO_2$, and $SO_4^=$ over the ocean to the south of Nova Scotia, Canada, has been determined for the summer season from in situ measurements. The instrumentation platform was the National Research Council of Canada Twin Otter aircraft, sampling at altitudes from 0.03 to 5 km.

Analysis of back trajectories shows that the air arriving at this location at 925 mbar and aloft had passed over regions of potentially high anthropogenic emission at least 50% of the time. Air arriving at the surface had passed through the cleaner northern continental regions or over the ocean 70% of the time. In the summer, air within the lowest 1 km of the atmosphere was generally stable, and there was a lack of forcing for convection. Strong wind speeds from the continent, and the release of pollutants in this region provided a mechanism for significant transport of pollutants out over the North Atlantic. This transport of pollutants was seen to occur aloft, with less-polluted air near the surface.

The average mass of $O_3$ transported eastward through a surface 1 m in horizontal extent and 5 km in the vertical is 2.8 g $s^{-1}$. The contribution of anthropogenic $O_3$ is estimated to account for 50% of the transport below 1 km, 35-50% from 1 to 3 km, 25-50% from 3 to 4 km, and 10% from 4 to 5 km. The average transport of $O_3$ due to anthropogenic sources though the surface as defined above is 0.86 g $s^{-1}$ from 264°.

The average mass of $SO_2$ and $SO_4^=$ transported through a surface 1 m in horizontal extent and 5 km in the vertical is 49 mg S $s^{-1}$, moving from west to east. These summertime observations show that more $SO_4^=$ is transported at higher altitudes than $SO_2$, consistent with enhanced conversion of $SO_2$ to $SO_4^=$ and vertical transport due to cloud processing. Substantial quantities of water vapour are being transported at the same altitudes as the $SO_4^=$.

These point measurements are generalized to longer distance and timescales to compare with earlier estimates of the flux of anthropogenically produced $O_3$ and S to the North Atlantic atmosphere. For a distance of 2000 km (measured along a meridian) 14 Tg of anthropogenically produced $O_3$ and 0.8 Tg of S are transported per summer out to the North Atlantic atmosphere.

**Acknowledgments.** The authors thank Steve Bacic of AES, and John Aitken, Murray Morgan, Chuck Taylor, Matthew Bastien, and other staff of the Institute for Aerospace Research for invaluable assistance in the field. We are grateful to Keith MacQuarrie and Tatiana Potylitsina for help in data processing, and to Peter Liu for help with the figures.

## References

Anderson, B.E., G.L. Gregory, J.D.W. Barrick, J.E. Collins, Jr., G.W. Sachse, D. Bagwell, M.C. Shipham, J.D. Bradshaw, and S.T. Sandolm, The impact of U.S. continental outflow on ozone and aerosol distributions over the western Atlantic, *J. Geophys. Res.*, *98*, 23,477-23,489, 1993.

Angevine, W.M., and J.I. MacPherson, Comparison of wind profiler and aircraft wind measurements at Chebogue Point, Nova Scotia, *J. Atmos. Oceanic Technol.*, *12*, 421-426, 1995.

Angevine, W.M., M. Trainer, S. McKeen, and C.M. Berkowitz, Mesoscale meteorology of the New England coast, Gulf of Maine and Nova Scotia: Overview, *J. Geophys. Res.*, this issue.

Benkovitz, C.M., C.M. Berkowitz, R.C. Easter, S. Nemesure, R. Wagener, and S.E. Schwartz, Sulfate over the North Atlantic and adjacent continental regions: Evaluation for October and November 1986 using a three-dimensional model driven by observation-driven meteorology, J. Geophys. Res., *99*, 20725-20756, 1994.

Berkowitz, C.M., K.M.Busness, E.G. Chapman, J.M. Throp, and R.D. Saylor, Observations of depleted ozone within the boundary layer of the western North Atlantic, *J. Geophys. Res.*, *100*, 11,483-11,496, 1995.

Daum, P.H., L.I. Kleinman, L. Newman, W. Luke, J. Weinstein-Lloyd, C.M. Berkowitz, and K. Busness, Chemical and physical properties of plumes of anthropogenic pollutants transported over the North Atlantic during the North Atlantic Regional Experiment, *J. Geophys. Res.*, this issue.

Fehsenfeld, F.C., S. Penkett, M. Trainer, and D.D. Parrish, NARE 1993 Summer Intensive: Forword, *J. Geophys. Res.*, this issue (a).

Fehsenfeld, F.C., P. Daum, W.R. Leaitch, M. Trainer, D.D. Parrish and G. Hubler, Transport of $O_3$ and $O_3$ precursors over the North Atlantic: An overview of the 1993 NARE summer intensive, *J. Geophys. Res.*, this issue (b).

Galloway, J.N., and D.M. Whelpdale, WATOX-86 overview, and western North Atlantic Ocean S and N atmospheric budgets, *Global Biogeochem. Cycles*, *1*, 261-281, 1987.

Husain, L., V.A. Dutkiewicz, M.M. Hussain, H.A. Khwaja, E.G. Burkhard, G. Mehmood, P.P. Parekh, and E. Canelli, A study of heterogeneous oxidation of $SO_2$ in summer clouds, *J. Geophys. Res.*, *96*, 18,789-18,805, 1991.

Isaac, G.A., W.R. Leaitch, and J.W. Strapp, The vertical distribution of aerosols and acid related compounds in air and cloud water, *Atmos. Environ.*, *24A*, 3033-3046, 1990.

Kleinman, L.I., and P.H. Daum, Vertical distribution of aerosol particles, water vapour and insoluble trace gases in convectively mixed air, *J. Geophys. Res.*, *96*, 991-1005, 1991.

Kleinman, L.I., P.H. Daum, Y.-N. Lee, S. R. Springston, L. Newman, W.R. Leaitch, C.M. Banic, G. A. Isaac, and J.I. MacPherson, Measurement of $O_3$ and related compounds over southern Nova Scotia, 1, Vertical distributions, *J. Geophys. Res.*, this issue (a).

Kleinman, L.I., P.H. Daum, S. R. Springston, W.R. Leaitch, C.M. Banic, G. A. Isaac, B.T. Jobson, and Hiromi Niki, Measurement of $O_3$ and related compounds over southern Nova Scotia, 2, Photochemical age and vertical transport, *J. Geophys. Res.*, this issue (b).

Leaitch, W.R., C.M. Banic, G.A. Isaac, M.D. Couture, P.S.K. Liu, I. Gultepe, S.-M. Li, L.I. Kleinman, P.H. Daum, and J.I. MacPherson, Physical and chemical observations in marine stratus during 1993 NARE: Factors controlling cloud droplet number concentrations, *J. Geophys. Res.*, this issue.

Li, S.-M., C.M. Banic, W.R. Leaitch, P.S.K. Liu, X.-L. Zhou, and Y.-N. Lee, Water soluble fractions of aerosol and their relation to number size distributions based on aircraft measurements from NARE 1993, *J. Geophys. Res.*, this issue.

Liu, P.S.K., W.R. Leaitch, A.M. Macdonald, G.A. Isaac, J.W. Strapp, and H.A. Wiebe, Sulphate production in summer cloud over Ontario, Canada, *Tellus*, *45*B, 368-390, 1993.

Luria, M., C.C. Van Valin, J.F. Boatman, D.L. Wellman, and R.F. Pueschel, Sulfur dioxide flux measurements over the western Atlantic Ocean, *Atmos. Environ.*, *21*, 1631-1636, 1987.

Luria, M., C.C. Van Valin, , W.C. Keene, D.L. Wellman, J.N. Galloway, and J.F. Boatman, Eastward sulfur flux from the northeastern United States, *Atmos. Environ.*, *22*, 1847-1854, 1988.

Olson, M.P., K.K. Oikawa, and A.W. MacAfee, A Trajectory Model Applied to the Long-Range Transport of Air Pollutants, *Rep. LRTAP 78-4*, Atmos. Environ. Ser., Air Quality Res. Branch, Downsview, Ontario, Canada, 1978.

Parrish D.D., J.S. Holloway, M. Trainer, P.C. Murphy, G.L. Forbes, and F.C. Fehsenfeld, Export of North American ozone pollution to the North Atlantic Ocean, *Science*, *259*, 1436-1439, 1993.

Seinfeld, J. H., *Atmospheric Chemistry and Physics of Air Pollution*, John Wiley, New York, 1986.

Tarrason, L., and T. Iversen, The influence of North American anthropogenic sulphur emissions over western Europe, *Tellus*, *44*B, 114-132, 1992.

Whelpdale, D.M., and J.N. Galloway, Sulfur and reactive nitrogen fluxes to the North Atlantic atmosphere, *Global Biogeochem. Cycles*, *8*, 481-493, 1994.

C.M. Banic, M.D. Couture, G.A. Isaac, W.R. Leaitch, Atmospheric Environment Service, Cloud Physics Research Division, 4905 Dufferin Street, Downsview, Ontario M3H 5T4 CANADA. (e-mail: armpcb1@dowsv01.dow.on.doe.ca; couture@armph3.dow.on.doe.ca; isaacg@am.dow.on.doe.ca; leaitch@armph3.dow.on.doe.ca)

L.I. Kleinman, S.R. Springston, Environmental Chemistry Division, Brookhaven National Laboratory, P.O. Box 5000, Upton, NY 11973-5000. (e-mail: kleinman@bnlcl6.bnl.gov; srs2@bnl.gov)

J.I. MacPherson, Institute for Aerospace Research, National Research Council, Montreal Road, Building U-61, Ottawa, Ontario K1A 0R6 CANADA. (e-mail: macpherson@iaruplands.lan.nrc.ca)

(Received May 15, 1995; revised October 17, 1995;
accepted October 17, 1995)